ORIGINAL ARTICLE

Fault diagnosis of rolling bearings in non-stationary running conditions using improved CEEMDAN and multivariate denoising based on wavelet and principal component analyses

Lilia Chaabi[1] · Ahcene Lemzadmi[1] · Abderrazek Djebala[2] · Mohamed Lamine Bouhalais[2] · Nouredine Ouelaa[2]

Abstract

This paper presents a fault diagnosis method for rolling bearings working in non-stationary running conditions. The proposed approach is based on an improved version of the improved complete ensemble empirical mode decomposition with adaptive noise (ICEEMDAN), the multivariate denoising using wavelet analysis and principal component analysis (PCA), the spectral kurtosis, and the order tracking analysis (OTA). The results show that the improved CEEMDAN has completely decomposed the raw signal into different intrinsic mode functions (IMFs) representing the natural oscillatory modes embedded into the signal. The most relevant IMF from which the defect was extracted is selected by the kurtogram plot which allows locating the optimal frequency band having the highest kurtosis value. Multivariate denoising based on wavelet analysis and PCA is used to increase the signal-to-noise ratio (SNR) of the selected IMF. The results show the great contribution of the denoising approach when comparing the selected denoised IMF with the original one. Finally, order tracking analysis is applied on the denoised IMF's envelope to remove the effect of speed variation, and an envelope order spectrum is obtained. The proposed approach is first applied on theoretical signal simulating rolling bearing defect in variable regime including three different phases. The final order spectrum shows exactly the simulated defect order and several of its harmonics. For the experimental validation, several signals of defective rolling bearings have been measured on the Machine Fault Simulator test rig in variable regime. Despite the combined variable regime including acceleration-constant regime-deceleration, at the same time, the obtained results indicate the efficiency of the proposed method to extract the fault order with high accuracy. The maximum error between the theoretical order and the experimentally obtained one was 1.3% for outer race defect and 1% for inner race defect. Finally, the performances of the proposed method are compared to those of another diagnosis method designed for variable regime conditions. Both outer race and inner race defects are considered in acceleration regime. The results show the superiority of the proposed method to highlight the defect order with highest clarity.

Keywords Rolling bearing faults · Non-stationary conditions · Improved CEEMDAN · Multivariate denoising · Principal component analysis · Order tracking analysis

1 Introduction

Rolling bearing is the most important part in any rotating machine. Damage of rolling bearing components can cause catastrophic failures that influence the running conditions of the machine and the whole production process. Despite the use of preventive maintenance management program based on theoretical calculations, the maintenance crew is often unable to predict the exact lifetime of the rolling bearing. Actually, the overloads applied on the bearing cause its destruction before scheduled date. The predictive maintenance based on vibratory analysis is then the most reliable technique used for rolling bearing monitoring and diagnosis in real time. Taking advantage of the development of signal processing techniques, several methods have been proposed these last years.

Among the powerful tools used for detection of rolling bearing faults, time-frequency approaches are the most recent.

✉ Abderrazek Djebala
djebala_abderrazek@yahoo.fr; djebala.abderrazek@univ-guelma.dz

1 Laboratory of Electrical Engineering of Guelma, May 8, 1945 University of Guelma, Guelma, Algeria

2 Laboratory of Mechanics and Structures, May 8, 1945 University of Guelma, Guelma, Algeria

These methods provide local analysis of the signal, instead of the global analysis given by the classical methods. In the last two decades, wavelet transform was undoubtedly the star in the time-frequency analysis of vibratory signals. Many researches applied several versions of the wavelet analysis for the detection of bearing defects [1–4]. Among the applications of wavelet analysis, denoising approaches have been widely used and discussed in the literature. Inspired from the well-known wavelet denoising proposed by Donoho [5], a new and effective approach is proposed in [6]. It uses a multivariate denoising based on wavelet analysis and principal component analysis. This new denoising method gave better results than those obtained by the classical soft or hard thresholding methods.

Wavelet analysis being non-adaptive, however, has its own disadvantage that their analysis results depend on the choice of the wavelet base function [7]. To overcome this limit, a self-adaptive analysis was proposed by Huang in 1998 [8] under the name of empirical mode decomposition (EMD). EMD was widely used for detection of rolling bearing faults alone [9–11] or combined with other signal processing tools [12–17].

Despite its efficiency, the EMD has the mode mixing problem, where we may find that different scales may be consisted in one oscillatory component, called intrinsic mode function (IMF), or that similar scales may reside in different IMFs, which could make individual IMF devoid of physical meaning and lead to false diagnostic. As solution to this problem, ensemble empirical mode decomposition (EEMD) was proposed in 2009 [18]. The main idea of the EEMD consists in adding white noise to the analyzed signal and calculating an ensemble of trials using the original EMD. The mean of the result of each ensemble represents the true IMF. By overcoming the mode mixing problem, the EEMD method provides more accuracy but, unfortunately, causes more computing time which represents its principal drawback. Despite this limitation, several applications used the EEMD for the detection of rolling bearing defects [19–21]. Moreover, EEMD has a second serious limitation that the residue of white noise still exists in the reconstructed components, because the added white noise is not completely removed from the IMFs by the averaging process.

For this reason, a new algorithm called complete ensemble empirical mode decomposition with adaptive noise (CEEMDAN) was initially proposed by Torres et al. in 2011 [22] and successfully applied on ECG signals. Contrary to EEMD, CEEMDAN provides complete decomposition with numerically negligible error. In CEEMDAN procedure, a particular noise is added at each stage of the decomposition and a unique residue is computed to obtain each IMF. Nevertheless, little noise still exists, leading to some *spurious* IMFs in the earlier decomposition.

An improvement of this technique is then proposed by Colominas et al. in 2014 [23] and also applied to analyze ECG signals. The improved CEEMDAN allows less residue of white noise and more physical meaning of the obtained IMFs. The main mathematical improvement consists in adding an IMF of the white noise decomposed by EMD at each stage, and a unique residue is then obtained. The true IMF is computed as the difference between the current residue and the average of its local means [24]. These techniques (CEEMDAN and improved CEEMDAN) have been applied in several papers for the detection of rolling bearing defects [25–28].

Unfortunately, most of these methods are ineffective to analyze signals measured in variable regime conditions. The necessity to monitor this type of machines via vibratory analysis incites the researchers to develop signal processing methods adapted from classical well-known techniques or simply propose new ones. Several researches investigated this field, but the published papers are still little compared to those treating the steady-state running conditions [25, 29–31].

The objective of this paper is to propose a new diagnosis method for rolling bearings running in variable regime using improved CEEMDAN, multivariate denoising based on wavelet analysis and PCA, spectral kurtosis, and order tracking analysis (OTA) (this method will be called later ICEEMDAN-MVD method). Section 2 is devoted to the presentation of the theoretical framework of the proposed method including the improved CEEMDAN and its predecessor versions (the multivariate denoising and the order tracking analysis). Simulation of rolling bearing defects in non-stationary running conditions is proposed in Section 3. The proposed approach methodology is detailed in Section 4 and applied on theoretical signal in Section 5. Experimental application on measured vibratory signals is carried out in Section 6. Comments and discussions of the obtained results are given in section 7. Finally, the proposed approach is compared to another diagnosis method in Section 8.

2 Theoretical foundations of the proposed method

2.1 EEMD, CEEMDAN, and improved CEEMDAN

To overcome the mode mixing problem of the EMD, the EEMD, being a noise-assisted analysis, was proposed. The EEMD calculates an ensemble of trials using the original EMD, adding in each trial a different realization of white noise of finite variance, i.e., random signal having equal intensity at different frequencies giving it a constant power spectral

density. The mean of the result of each ensemble represents the true IMF. This can be summarized as follows [18, 25]:

1. Generate $x^i(t) = x(t) + w^i(t)$, where $x(t)$ is the original signal and $w^i(t)$ [$i = 1, ..., I$] is the different realizations of white Gaussian noise
2. Each $x^i(t)$ is decomposed by EMD getting its modes $IMF_k^i(t)$, where $k = 1, ..., I$ indicates the modes
3. Assign $\overline{IMF_k}$ as the kth mode of $x(t)$, obtained as the average of the corresponding $\overline{IMF_k(t)} = \frac{1}{I} \sum_{i=1}^{I} IMF_k^i(t)$

The main problem of the EEMD is the high computing time and the residue of added noise present in the IMFs. To overcome this limitation, the CEEMDAN algorithm was first proposed by Torres et al. in 2011 [22]. The main idea of the CEEMDAN is to add white noise in a specific frequency band during the decomposition. CEEMDAN uses the same EEMD algorithm to calculate the first mode function $\overline{IMF_1}$ only, and a unique first residue is then calculated as

$$r_1(t) = x(t) - \overline{IMF_1(t)} \tag{1}$$

Then, compute the EMD mode over an ensemble $r_1(t)$ plus different realizations of a given noise, obtaining $\overline{IMF_2}(t)$ by averaging. $r_2(t)$ is then calculated as

$$r_2(t) = r_1(t) - \overline{IMF_2(t)} \tag{2}$$

This step is repeated with the other modes until the stopping criterion is reached.

In order to summarize the procedure of CEEMDAN, $E_j(.)$ is defined as an operator which, given a signal, produces the jth mode obtained by EMD, and ε_i represents the signal-to-noise ratio (SNR); the steps of the technique are the following:

1. Decompose I realizations of $x(t) + \varepsilon_0 \, w^i(t)$ by EMD to obtain the first $\overline{IMF_1}$ by averaging

$$\overline{IMF_1(t)} = \frac{1}{I} \sum_{i=1}^{I} IMF_1^i(t) \tag{3}$$

2. Calculate the first residue as

$$r_1(t) = x(t) - \overline{IMF_1(t)} \tag{4}$$

3. Decompose I realizations of $r_1(t) + \varepsilon_1 \, E_1(w^i(t))$ until their first EMD mode and calculate the second mode

$$\overline{IMF_2(t)} = \frac{1}{I} \sum_{i=1}^{I} E_1 \left(r_1(t) + \varepsilon_1 \, E_1 \left(w^i(t) \right) \right) \tag{5}$$

4. For $k = 2, ..., K$, calculate the kth residue

$$r_k(t) = r_{k-1}(t) - \overline{IMF_k(t)} \tag{6}$$

5. For $k = 2, ..., K$, define the $(k + 1)$th mode as

$$\overline{IMF_{k+1}(t)} = \frac{1}{I} \sum_{i=1}^{I} E_1 (r_k(t) + \varepsilon_k \, E_k(w(t))) \tag{7}$$

6. Go to step 4 for next k

Steps from 4 to 6 are repeated until the obtained residue is no longer feasible to be decomposed and satisfies

$$R(t) = x(t) - \sum_{k=1}^{K} \overline{IMF_k}(t) \tag{8}$$

where K is the total number of modes. The original signal $x(t)$ can be expressed in the end as

$$x(t) = \sum_{k=1}^{K} \overline{IMF_k}(t) + R(t) \tag{9}$$

Even with the CEEMDAN algorithm, little residue of added white noise still exists in the obtained IMFs. Improved CEEMDAN is then proposed by Colominas et al. in 2014 [23]. Applied on theoretical and ECG real signals, the new improved version is presented to be more effective than all the previous versions. The improved CEEMDAN algorithm is summarized as [23]

1. Calculate the local means of l realizations using the EMD algorithm: $x^i(t) = x(t) + \varepsilon_0 \, E_1(w^i(t))$ and obtain the first residue: $r_1(t) = (M(x^i(t)))$, where $M(.)$ is the operator which produces the local means of the signal and w^i is a realization of white noise
2. Calculate the first IMF as $\overline{IMF_1}(t) = x(t) - r_1(t)$
3. Estimate the second residue as the average of local means of the realizations $(r_1(t) + \varepsilon_1 \, E_2(w^i(t)))$ and calculate the second IMF as $\overline{IMF_2}(t) = r_1(t) - r_2(t)$
4. Calculate the kth IMF: $IMF_k(t) = r_{k-1}(t) - r_k(t)$
5. Go to step 4 for next k

2.2 Multivariate denoising using wavelet analysis and PCA

This new algorithm combines the well-known wavelet denoising procedure widely used in the literature and principal component analysis. The denoising procedure is as [6]

1. Perform the wavelet transform at level J of each column of $x(t)$
2. For $1 \leq j \ll J$, perform the PCA of the detail matrix D_j and select an appropriate number (p_j) of useful principal component or suppress the detail D_j
3. Do again step 2 for the approximations of matrix A_j
4. Reconstruct the new matrix $\overset{\vee}{x}$ by the inverse wavelet transform from the simplified details and approximations
5. Perform the PCA of matrix $\overset{\vee}{x}$ and build adequate statistic for statistical process control (SPC)

2.3 Order tracking analysis

The monitoring of bearing defects is more complicated when the operating parameters of the system are variables, in particular for speed and load. The analysis of vibratory signals in this case is often preferred in terms of order spectrum rather than frequency spectrum. In the frequency domain, the data must be sampled at constant time intervals. For the order tracking analysis, it is necessary to sample the vibration signal at constant angular increments and, therefore, at a rate proportional to the shaft speed. This is achieved using analog instrumentation.

In stationary regime, the detection of the bearing defect type returns to look for its characteristic frequency in the spectrum (BPFO, BPFI, BSF, FTF). As well known, these characteristic frequencies are calculated in function of the bearing geometry and the rotation speed. In the case of non-stationary conditions, the rotation speed is variable, and these characteristic frequencies are also variables. It is then almost impossible to detect the defect by the conventional approaches. The defect characteristic frequencies can then be simplified as

Defect characteristic frequency (Hz) $= N.C_j$ with $j = 1:4$

where C_1, C_2, C_3, and C_4 are constants (which will be later called defect orders) determined from the bearing geometry and N is the rotation speed. As solution to non-stationary effect, it is therefore common to look for these constants (orders) rather than the characteristic frequencies which are variables. For this, we must perform an order spectrum rather than a frequency spectrum.

3 Simulation of rolling bearing defects in variable regime

The signal of defective rolling bearing is characterized by periodical impulse train. Each impulse is modulated by a single harmonic frequency with exponential decay as shown in Eq. (10):

$$s(t) = e^{-\alpha t}\sin(2\pi f_r t) \tag{10}$$

where α is the damping ratio of the impulse and f_r is the resonance frequency of the bearing.

The period between two successive impulses represents the defect characteristic frequency that depends on the defect type. This model has been widely used in the literature to test different diagnosis methods [1, 2, 32, 33].

In the non-stationary case, the fault frequencies are variable and follow the speed variation, which means that the periods between impulses are unequal. If it is an acceleration, the periods are going to decrease while speeding up. On the other hand, the periods between impulses are going to increase in the case of deceleration. In practice, bearing signals are often contaminated with noise and modulated either by shaft speed, cage speed, or their difference, depending on the location of the fault [25]. It is also often that a time lag between impulses occurs due to the slippage of the rolling elements between the two bearing rings. The final obtained signal can be then mathematically expressed as

$$x(t) = \sum_i A_i h(n - iT - \tau_i) + n(t) \tag{11}$$

where A_i is the amplitude modulation of the ith impact force, T is the period between two successive impacts, τ is the time lag produced by the slip, $h(.)$ is the impulse response, and $n(t)$ is the white Gaussian noise. The adopted model has been successfully used in previous literature to represent bearing signals working in variable speed [25, 30, 34].

As example, Fig. 1 a represents a signal simulating rolling bearing defect in the case of an acceleration. Figure 1b shows the same signal after adding a variable level of white noise. The bearing natural frequency is taken equal to 2800 Hz, and the defect characteristic frequency increases from 100 to 300 Hz. If we assume a defect order equal to 3, the rotation speed increases from 33.3 Hz (2000 RPM) to 100 Hz (6000 RPM). To clearly illustrate the effect of the acceleration on the impacts' amplitude and its period and on the added noise, we took a small number of samples. A much higher number of samples (as in the measured signals) mean very high computing time and will not illustrate the variable regime, properly.

The application of the well-known demodulation technique (still called envelope analysis or high-frequency resonance technique) around the natural frequency allows obtaining the envelope spectrum of Fig. 2. No information can be obtained, and the peaks present in the envelope spectrum do not correspond to any known frequency.

4 Proposed approach methodology

The proposed approach procedure contains four main steps:

Fig. 1 Signal simulating rolling bearing defect in acceleration regime. **a** Pure signal. **b** Noisy signal
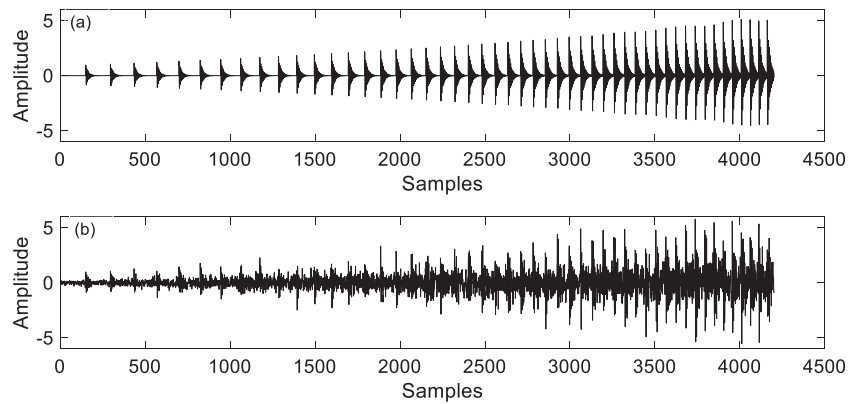
a. First step: Decompose the signal by the improved CEEMDAN

It is well known that a signal measured on rotating machine reflects its vibratory state. The problem is that this raw signal contains different frequency components. These frequency components correspond to different vibratory phenomena generated by the machine parts at the same time (shafts, bearings, gears, coupling, electrical motor, etc.). To get information about the occurrence of specific defect, it is imperative to extract its signature from the raw signal, and this is not usually obvious.

For this, the proposed ICEEMDAN-MVD method uses the improved CEEMDAN to decompose the signal into several IMFs. As complete decomposition, the ICEEMDAN will isolate the signature of the rolling bearing defect in specific IMF.

b. Second step: Perform kurtogram plot and select the optimal frequency band

After decomposing the signal into different IMFs, the question is which IMF contains the signature of rolling bearing defect. A rolling bearing defect excites the structure in high frequency range, and the bearing natural frequency will be modulated by the defect characteristic frequency. The first IMFs (probably IMF1 or IMF2) must contain the signature of rolling bearing defect since it corresponds to high frequency range. It is then capital to look for a rational criterion to select the optimal IMF from which the defect can be extracted. As rolling bearing defects generate periodic chocks, the most reliable criterion is that sensitive to the impulsive forces. Through several papers in the literature, the kurtosis has been shown as the most sensitive indicator to detect mechanical defects inducing periodical shocks.

For this, in the second step of the proposed method, a kurtogram plot is performed using the fast spectral kurtosis algorithm established by Antoni [34]. It allows locating the best frequency band allowing the highest kurtosis value.

c. Third step: Compute FFT spectra of all the IMFs and perform multivariate denoising

In this step, the FFT spectra of all the obtained IMFs are calculated. The objective is to isolate the IMF covering the optimal frequency band selected by the kurtogram. The IMFs corresponding to low-frequency components will be automatically removed. As second confirmation of the optimal IMF's choice, the multivariate denoising approach based on wavelet

Fig. 2 Envelope spectrum of the noisy signal using HFRT
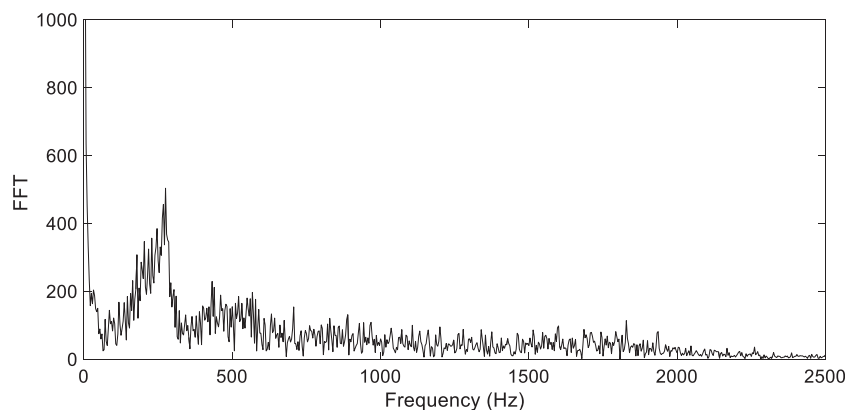
analysis and PCA methods is applied. The SNR of the selected IMF will be considerably improved and makes it possible to give final confirmation and more accuracy.

d. Fourth step: Apply order tracking analysis and perform envelope order spectrum

The most relevant IMF is being selected, and another problem still exists. Actually, this IMF was selected from a signal measured in non-stationary condition. It is almost impossible to extract the rolling bearing defect without removing the effect of speed variation. The proposed solution consists in using order tracking analysis on this IMF's envelope. An envelope order spectrum is then obtained instead of an envelope frequency spectrum as in the case of steady-state condition. The obtained envelope order spectrum will highlight the defect order and several of its harmonics.

NB. Steps 1 and 2 can be inverted without affecting the final result.

Fig. 3 Global flow chart of the proposed method

Fig. 4 Noisy signal simulating rolling bearing defect in variable regime (acceleration-constant regime-deceleration) with simulated defect order equal to 3

5 Application on simulated signal

The proposed ICEEMDAN-MVD approach is first applied on the simulated signal of Fig. 4. This signal is more complicated than that in Fig. 1 since it contains three phases: an acceleration from 33.3 Hz (2000 RMP) to 100 Hz (6000 RPM) in the first phase, a constant rotation speed at 100 Hz (6000 RPM) in the second phase, and finally, a deceleration from 100 Hz (6000 RPM) to 33.3 Hz (2000 RPM) in the third phase. In all the considered phases, the defect order is taken equal to 3. Consequently, the defect characteristic frequency ranges between 100 and 300 Hz. The bearing natural frequency is still taken equal to 2800 Hz.

Figure 5 shows the FFT spectrum that reveals the simulated natural frequency (2800 Hz). The calculation of the spectral kurtosis using the fast algorithm detailed in [33] allows obtaining the kurtogram in Fig. 6. The kurtogram shows that the optimal frequency band having the highest kurtosis ranges

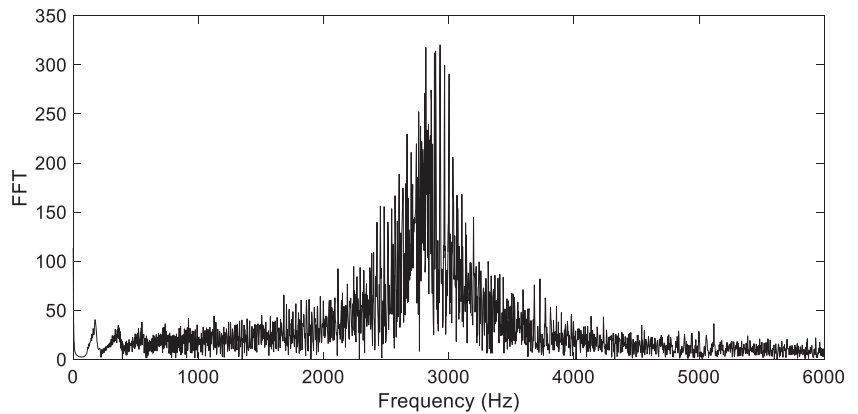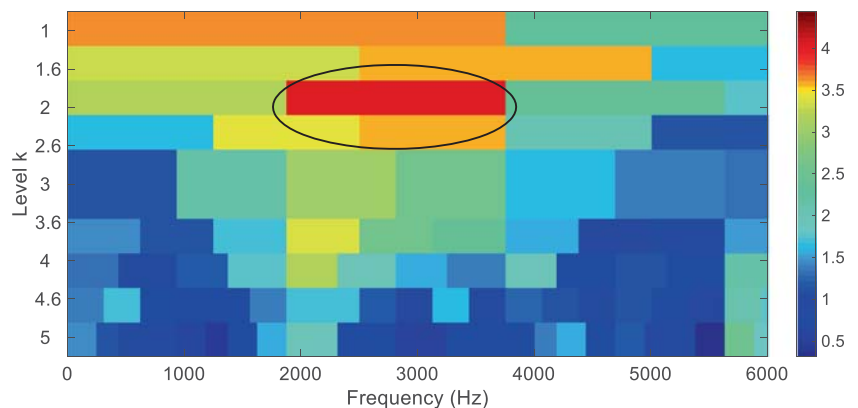**Fig. 5** FFT spectrum of the simulated signal

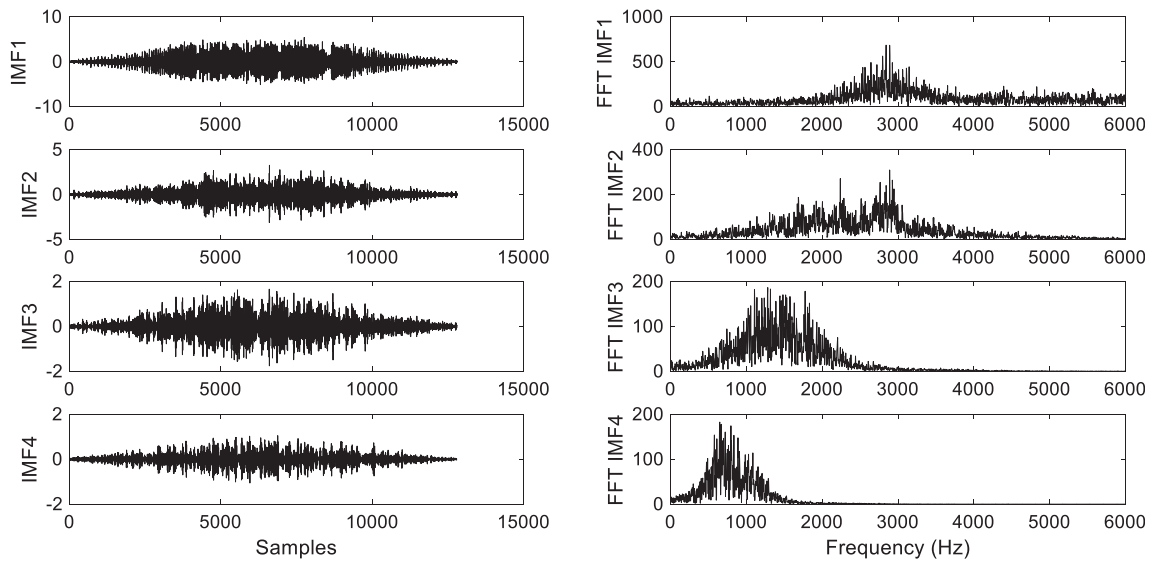**Fig. 6** Kurtogram of the simulated signal

Fig. 7 First four IMFs and its spectra obtained after the application of the improved CEEMDAN on the simulated signal

between 1900 and 3700 Hz with a center frequency at 2800 Hz, equal to the simulated natural frequency. This frequency band is then the best one revealing the periodical impacts generated by the simulated bearing defect.

Then, the improved CEEMDAN approach is applied, decomposing the simulated signal into several intrinsic mode functions. Figure 7 shows the first four IMFs and their spectra. The other IMFs correspond to low-frequency components and do not have a significant contribution in the defect detection. As first observation, IMF3 and IMF4 are automatically removed since they contain frequency components lower than the optimal frequency band. On the other hand, spectra of IMF1 and IMF2 show frequency modulations around the frequency band selected

from the kurtogram (1900 Hz to 3700 Hz), with advantage for the IMF1 highlighting more concentrated modulations. IMF1 seems the most relevant mode from which the defect can be extracted. This conclusion will be confirmed after performing the multivariate denoising.

As next step of the proposed method, multivariate denoising based on wavelet and principal component analyses is realized on the four IMFs obtained from the improved CEEMDAN. Figure 8 shows the four denoised IMFs, confirming with no confusion that the denoised IMF1 is the most relevant since it has a very significant kurtosis (21.72). The contribution of the denoising method is very obvious, and periodical impacts generated from the simulated defect are very clear.
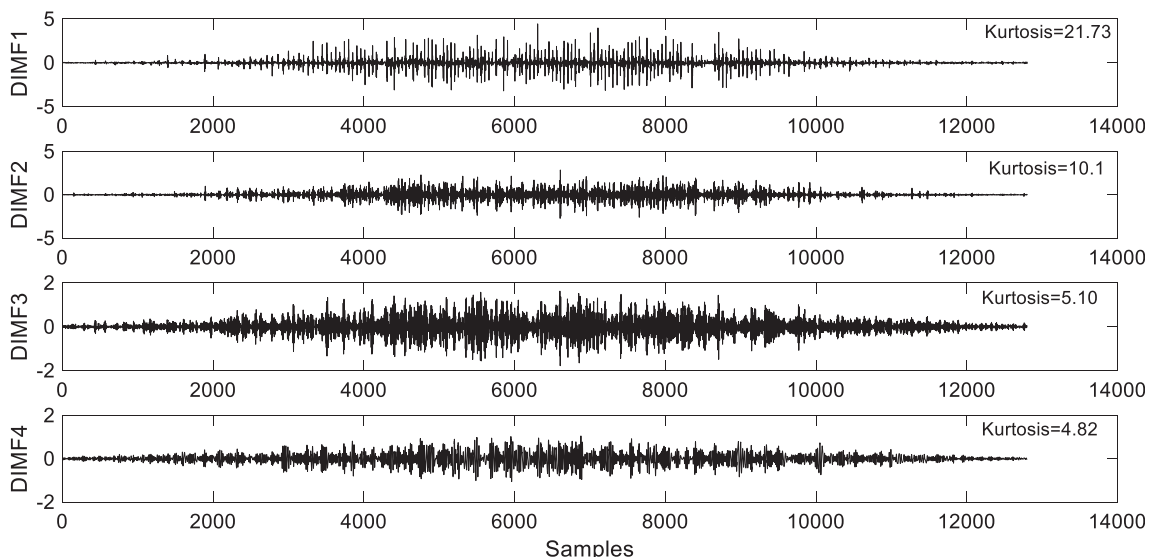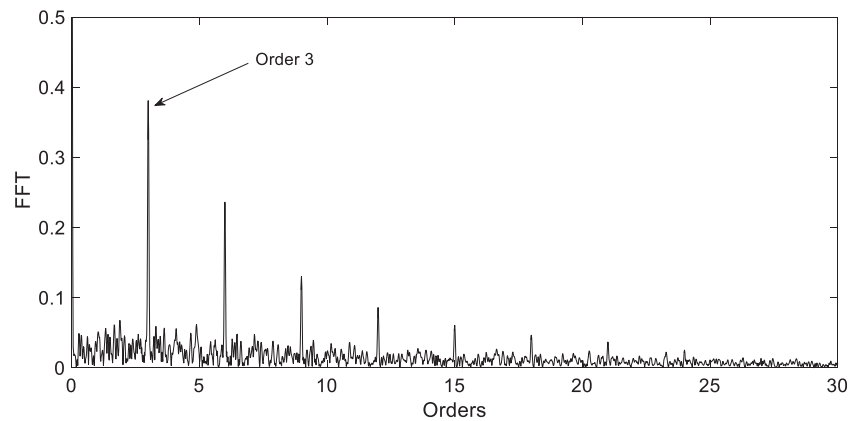

Fig. 8 Denoised IMFs obtained after the application of the multivariate denoising approach

Fig. 9 Envelope order spectrum of the denoised IMF1 obtained from the order tracking analysis (simulated defect order = 3)

Finally, order tracking analysis is applied on the envelope signal of the denoised IMF1 to remove the effect of speed variation. Figure 9 shows the order spectrum highlighting the simulated defect order (3) and several of its harmonics.

6 Experimental validation

In order to prove the efficiency of the proposed method in practice, several signals have been measured on a laboratory test rig in variable speed regime. The test rig is SpectraQuest® Machine Fault Simulator (MFS) as described in Fig. 10. The MFS is equipped with a kit of defective bearings having single point defects on outer race, inner race, and ball (combined defect is also available). The machine is also equipped with an automatic speed variator, allowing signal measurement in both constant and variable regimes. The signals are collected by accelerometers mounted on the bearing housing. The instantaneous rotation speed is measured simultaneously with vibratory signals via a tachometer. All collected data are then transferred to a 16-channel acquisition card in a PC. The post-treatment is carried out on Matlab® environment.

The proposed method is applied on the signal in Fig. 11 measured on a bearing with outer race defect. According to the bearing's geometry, the defect order is equal to 3.048. As for the simulated signal, the measured signal contains three phases: an acceleration from 0 to 1800 RPM, a constant speed at 1800 RPM, and finally, a deceleration from 1800 to 0 RPM. The signal contains 1,068,186 points and sampled at 15360 Hz.

Figure 12 shows the FFT spectrum of the measured signal, some modulations due to the system's natural frequencies are visible, and the most relevant modulation cannot be known without performing the kurtogram plot. Figure 13 shows the kurtogram of the measured signal obtained after the

Fig. 10 Machine Fault Simulator

Fig. 11 Signal of outer race defect measured in variable regime (acceleration-constant regime-deceleration) with theoretical defect order equal to 3.048
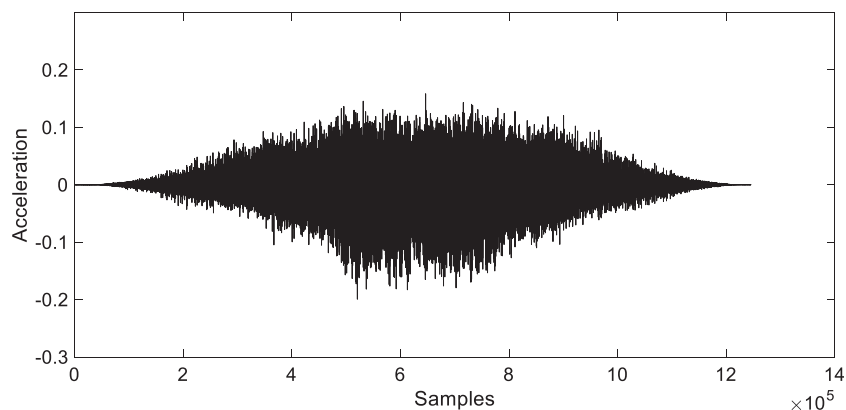
calculation of the spectral kurtosis, showing that the optimal frequency band ranges between 2200 and 2500 Hz with a center frequency around 2350 Hz.

The improved CEEMDAN is then applied on the measured signal, and Fig. 14 shows the first four IMFs and their corresponding spectra. As for the case of simulated signal, IMF3 and IMF4 are immediately removed, and their spectra correspond to low-frequency components. IMF1 and IMF2 are then taken as first selection since their spectra cover the optimal frequency band selected by the kurtogram. The multivariate denoising approach based on wavelet analysis and PCA is applied on the four IMFs. One can note that the kurtosis of the denoised signals of IMF1 and IMF2 is close (28 for IMF1 and 23 for IMF2). To remove the confusion about the most relevant IMF's selection, FFT spectra of all the denoised IMFs are performed. According to Fig. 15, the denoised signal of IMF2 is the relevant one since its spectrum covers the optimal frequency band selected by the kurtogram. Even if the kurtosis of the denoised IMF1 is little higher than that of denoised IMF2, its spectrum does not properly cover the optimal frequency band.

Order tracking analysis is finally applied on the envelope of the denoised signal (DIMF2), allowing the order envelope spectrum of Fig. 16. The spectrum highlights a main component corresponding to the order 3.09 and several of its

harmonics. This order is very close to the outer race defect order of the used rolling bearing (3.048) with an error of 1.3%. Moreover, this order spectrum is clearer than that obtained from the denoised IMF1 (Fig. 17) which confirms the assumption put before.

7 Comments and discussion on the obtained results

From the obtained results, some comments must be emphasized

1. Both theoretical simulation and experimental validations confirm that the improved CEEMDAN allows complete decomposition of the analyzed signal. The obtained IMFs have more physical meaning than those for EEMD analysis, for example. The disadvantage of the improved CEEMDAN resides in the high computing time, especially for signals having a high number of samples. For this, we noticed that beyond certain ensembles' number, there is no difference in terms of result accuracy. Between 10 and 100 ensembles, no significant difference was obtained; contrariwise, the difference between the computing times was immense.

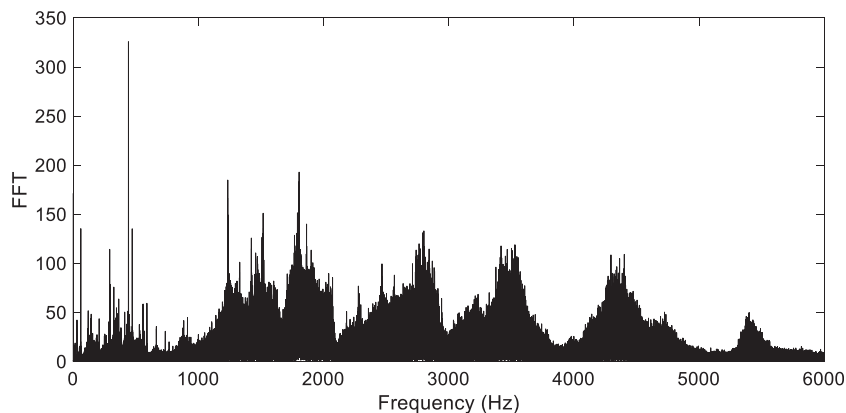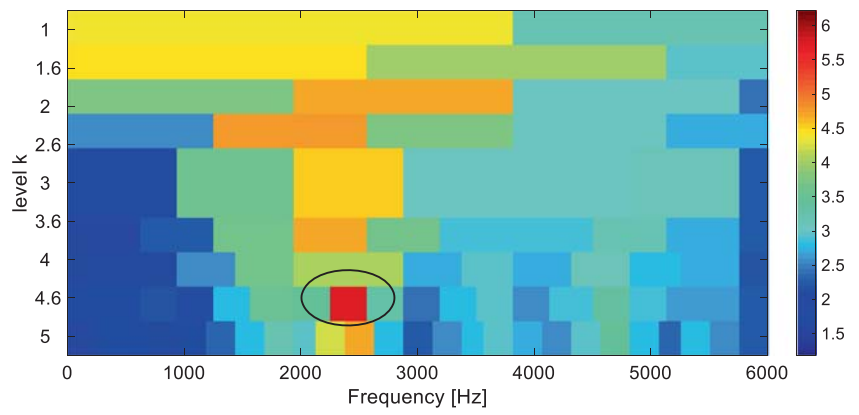**Fig. 12** FFT spectrum of the measured signal

Fig. 13 Kurtogram of the measured signal

2. Spectral kurtosis is proposed for the selection of the most relevant IMF. The kurtogram plot allows revealing, in very clear way, the optimal frequency band having the highest kurtosis value. The IMF from which the defect
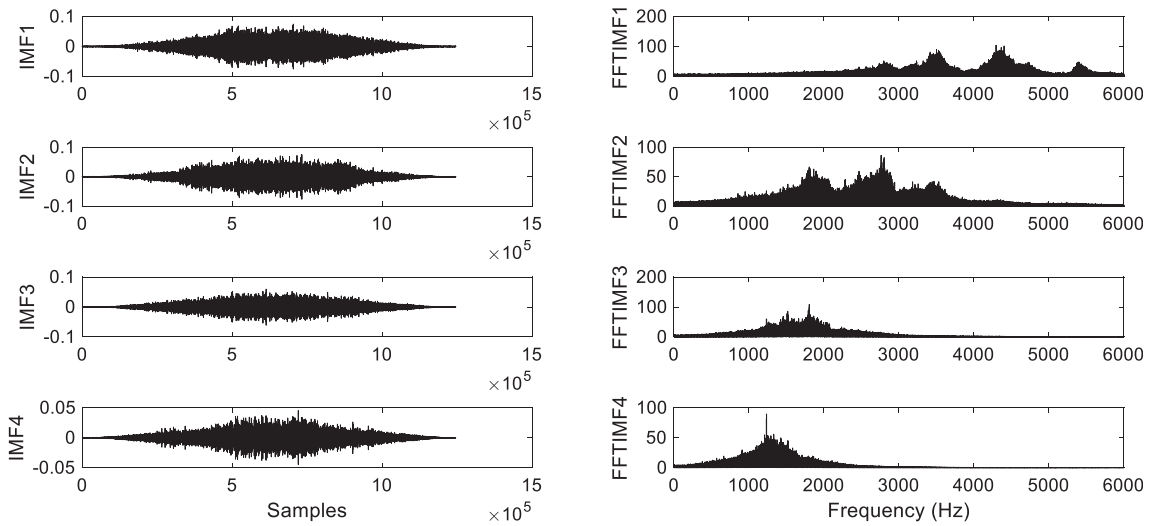

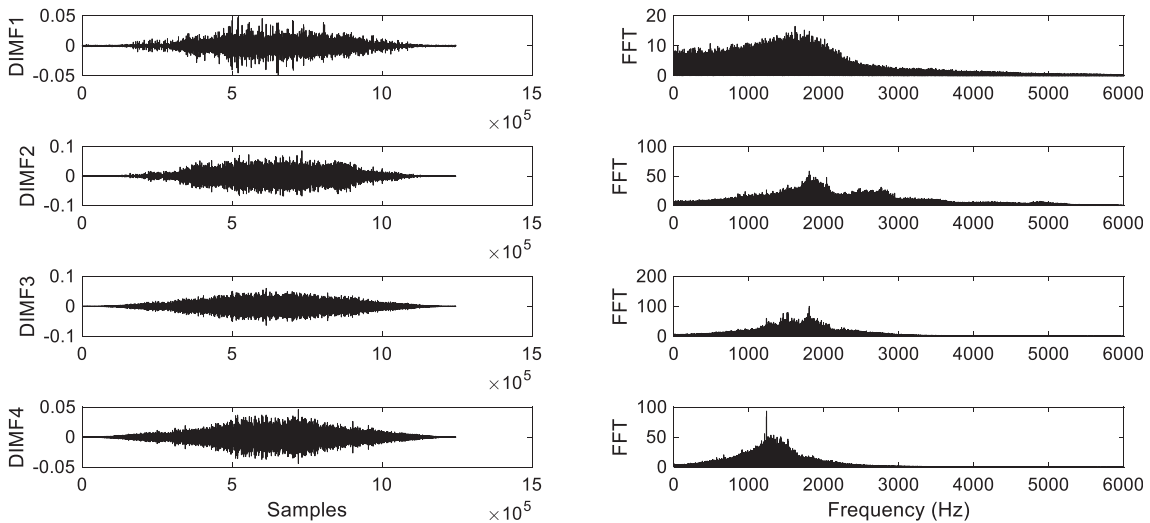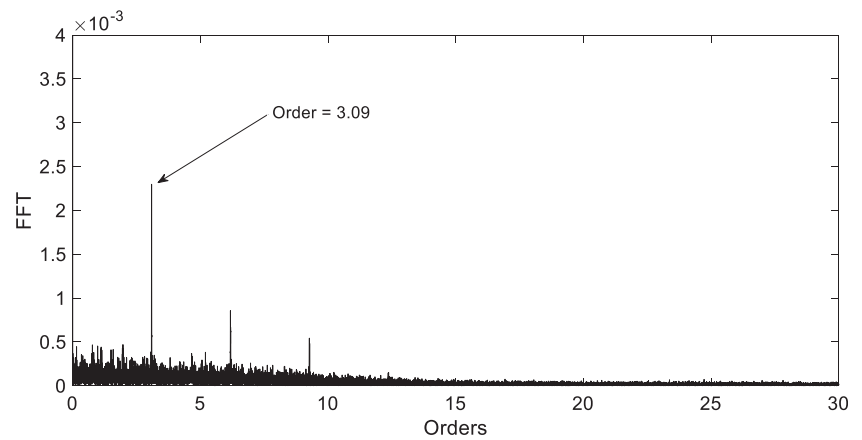**Fig. 14** First four IMFs and its spectra of the measured signal

Fig. 15 Denoised IMFs and its spectra

Fig. 16 Envelope order spectrum of the outer race defect in variable regime obtained from the denoised IMF2 (theoretical outer race defect order = 3.048)

can be extracted must imperatively cover this frequency band. In this context, it is important to mention that this approach only validates for the mechanical defects inducing periodical impulses (like rolling bearing and gear defects). For other defects, specific criteria must be found, tested, and applied.

3. To our knowledge, the pairing of multivariate denoising based on wavelet analysis and PCA and on the

ICEEMDAN method for the detection of rolling bearing defects in variable regime is original. Actually, the IMFs obtained from improved CEEMDAN (especially the relevant one) still contain little level of white noise. The contribution of the multivariate denoising was high efficacy when comparing the original relevant IMF with the denoised one. This step has considerably improved the

Fig. 17 Envelope order spectrum of the outer race defect in variable regime obtained from the denoised IMF1 (theoretical outer race defect order = 3.048)
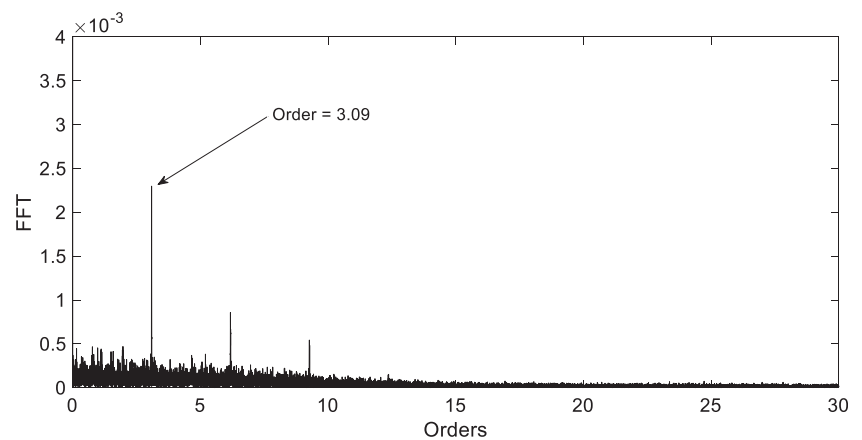
Fig. 18 Envelope order spectrum obtained from the proposed method for outer race defect (theoretical outer race defect order = 3.048)
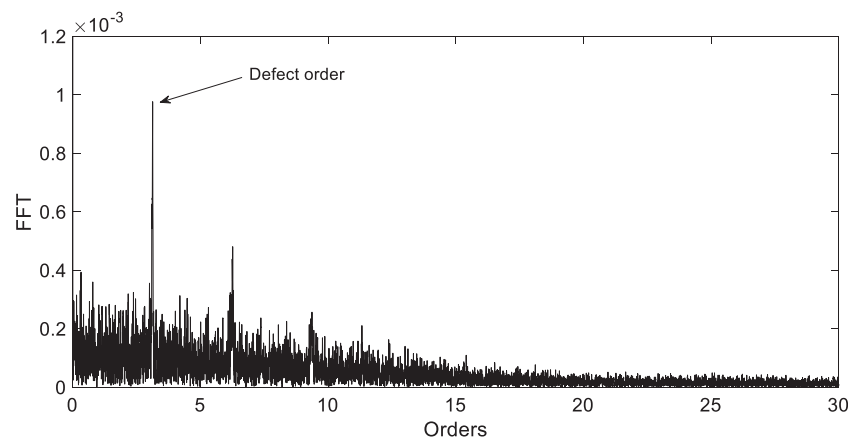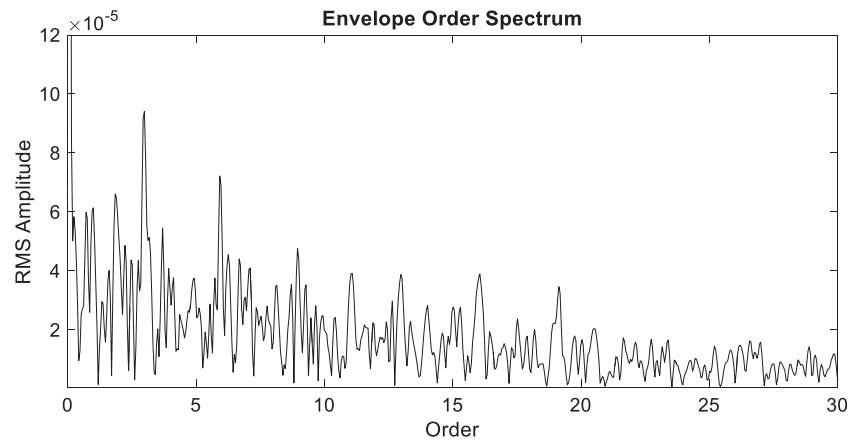
Fig. 19 Envelope order spectrum obtained from the CEEMDAN-WMRA method for outer race defect [25] (theoretical outer race defect order = 3.048)

clarity of the order spectrum obtained by the OTA method and then the diagnosis accuracy.

4. The proposed ICEEMDAN-MVD method uses order tracking analysis on the envelope of the relevant IMF instead of the IMF itself. The final spectrum is an envelope order spectrum that highlighted, in both simulation and experience, the defect order with high accuracy. It is very important to notice that this step gives accurate results, and RPM signal measured by the tachometer (or RPM vector in the case of simulation) must be carefully introduced simultaneously with the vibratory measured signal.

8 Comparison with another diagnosis method

The proposed method is compared to another diagnosis method designed for the detection of rolling bearing defects in variable regime. This method has been presented in [25], and it is a hybrid approach combining the original CEEMDAN and wavelet multiresolution analysis (WMRA). In this method, the signal is decomposed by the CEEMDAN

and the most relevant IMF is select by the calculation of the kurtosis. The WMRA is then applied on the selected IMF, and a reconstructed signal is built from the WMRA decomposition details (corresponding to high-frequency components). Order tracking analysis is then applied to get order spectrum. The comparison concerns the same signals presented in [25], i.e., outer race and an inner race defect signals measured in acceleration regime. Just the final envelope order spectrum is presented as comparison.

The first comparison concerns a signal measured on a bearing with outer race defect in acceleration regime. Figures 18 and 19 show the envelope order spectra obtained from the proposed method and the CEEMDAN-WMRA method, respectively. Without confusion, the order defect is clearly highlighted by the order spectrum obtained from the proposed method. Only the peaks corresponding to the defect order and its harmonics are visible, contrary to the CEEMDAN-WMRA method where the order spectrum is disturbed by frequency components making the defect order detection less obvious.

The second comparison is carried out on a signal of inner race defect in acceleration regime. According to the bearing's geometry, the defect order is equal to 4.95. Figure 20 shows

Fig. 20 Envelope order spectrum obtained from the proposed method for inner race defect (theoretical inner race defect order = 4.95)
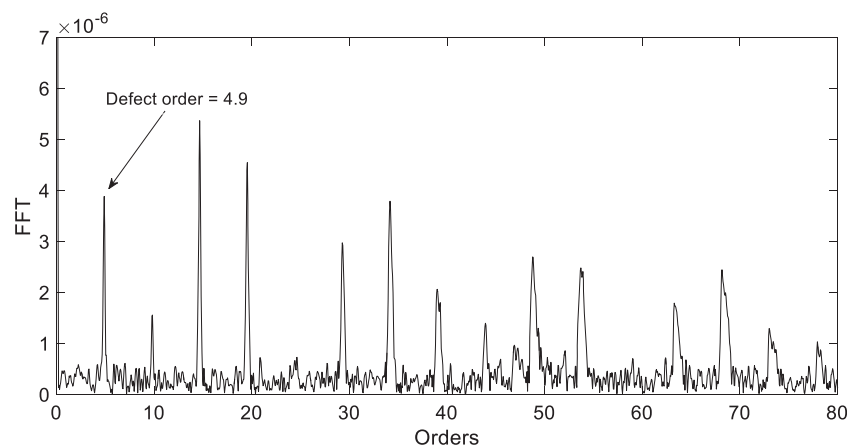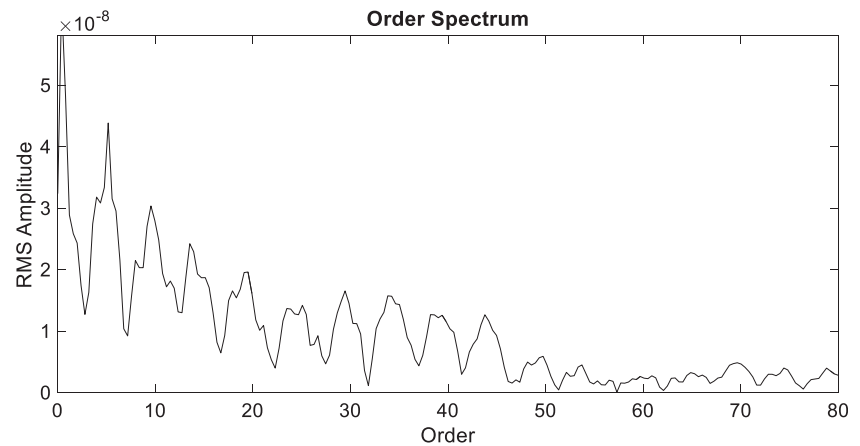
Fig. 21 Envelope order spectrum obtained from the CEEMDAN-WMRA method for inner race defect [25] (theoretical inner race defect order = 4.95)

the result obtained from the proposed method. A main order of 4.9 and some of its harmonics are clearly identifiable, very close to the inner race defect order with an error of 1%. The defect order is highlighted more clearly than in the order spectrum provided by the CEEMDAN-WMRA method (Fig. 21).

9 Conclusion

In this paper, a diagnosis method designed for the detection of rolling bearing defects in non-stationary running conditions is proposed. The proposed method is based on an improved complete ensemble empirical mode decomposition with adaptive noise, the multivariate denoising based on wavelet and principal component analyses, the spectral kurtosis, and order tracking analysis. The proposed method is shown to be very effective in the detection of the defect order in both simulated and experimental signals measured on defective rolling bearings in variable regime. For the simulation, the defect order has been exactly highlighted by the envelope order spectrum. For experimentation realized on bearings with single point defects in combined variable regime including three phases at the same time, the final order spectrum highlighted the defect order with an error of 1.3% for outer race defect and 1% for inner race one.

A comparison with another diagnosis method confirms the great advantage using the proposed method. The defect order is clearly detected in both outer race and inner race faults compared to the order spectrum obtained from the CEEMDAN-WMRA method. Note that the proposed approach is very simple to implement in an automatic diagnosis system. Despite that the mathematical foundations and the calculation programs are hard to understand by maintenance engineers, the final order spectrum is so simple that any member of the maintenance crew can interpret.

References

1. Djebala A, Ouelaa N, Hamzaoui N (2007) Optimisation of the wavelet multiresolution analysis of shock signals: application to the signals generated by defective rolling bearings. Mech Industry 4(8):379–389
2. Djebala A, Ouelaa N, Hamzaoui N (2008) Detection of rolling bearing defects using discrete wavelet analysis. Meccanica 43: 339–348
3. Yan R, Gao RX, Chen X (2014) Wavelets for faults diagnosis of rotary machines: a review with applications. Signal Process 96:1–15
4. Abouelanouar B, Elamrani M, Elkihel B, Delaunois F (2018) Application of wavelet analysis and its interpretation in rotating machines monitoring and fault diagnosis. A review. Int J Eng Technol 7(4):3465–3471
5. Donoho DL (1995) De-noising by soft thresholding. IEEE Transact Inform Theory 41(3):613–627
6. AminGhafari M, Cheze N, Poggi JM (2006) Multivariate denoising using wavelets and principal component analysis. Comput Stat Data Anal 52(6):3061–3074
7. Lei Y, Lin J, He Z, Zuo MJ (2013) A review on empirical mode decomposition in fault diagnosis of rotating machinery. Mech Syst Signal Process 35:108–126
8. Huang NE et al (1998) The empirical mode decomposition method and the Hilbert spectrum for non-stationary time series analysis. Proc Roy Soc London 454A:903–995
9. Dybala J, Zimroz R (2014) Rolling bearing diagnosing method based on empirical mode decomposition of machine vibration signal. Appl Acoust 77:195–203
10. Du Q, Yang S (2007) Application of the EMD method in the vibration analysis of ball bearings. Mech Syst Signal Process 21:2634–3644
11. Gao Q, Duan C, Fan H, Meng Q (2008) Rotating machine fault diagnosis using empirical mode decomposition. Mech Syst Signal Process 22:1072–1081
12. Bin GF, Gao JJ, Li XJ, Dhillon BS (2012) Early faults diagnosis of rotting machinery based on wavelet packets—empirical mode decomposition feature extraction and neural network. Mech Syst Signal Process 27:696–711
13. Pan MC, Tsao WC (2013) Using appropriate IMFs for envelope analysis in multiple fault diagnosis of ball bearings. Int J Mech Sci 69:114–124
14. Liu X, Lin B, Luo H (2015) Bearing faults diagnostics based on hybrid LS-SVM and EMD method. Measurement 59:145–166

15. Ahn JH, Kwak DH, Koh BH (2014) Fault detection of a roller-bearing system through the EMD of a wavelet denoised signal. Sensors 14(8):15022–15038

16. Djebala A, Babouri MK, Ouelaa N (2015) Rolling bearing fault detection using a hybrid method based on empirical mode decomposition and optimized wavelet multi-resolution analysis. Int J Adv Manuf Technol 79(9–12):2093–2105

17. Abdelkader R, Kaddour A, Derouiche Z (2018) Enhancement of rolling bearing fault diagnosis based on improvement of empirical mode decomposition denoising method. Int J Adv Manuf Technol 97(5–8):3099–3117

18. Wu Z, Huang NE (2009) Ensemble empirical mode decomposition: a noise-assisted data analysis method. Adv Adapt Data Anal 1(01): 1–41

19. Wu TY, Chung YL (2009) Misalignment diagnosis of rotating machinery through vibration analysis via the hybrid EEMD and EMD approach. Smart Mater Struct 18(9):095004

20. Guo W, Tse Peter W, Djordjevich A (2012) Faulty bearing signal recovery from large noise using a hybrid method based on spectral kurtosis and ensemble empirical mode decomposition. Measurement 45(5):1308–1322

21. Zhang X, Zhou J (2013) Multi-fault diagnosis for rolling element bearings based on ensemble empirical mode decomposition and optimized support vector machines. Mech Syst Signal Process 41: 127–140

22. Torres ME, Colominas MA, Schlotthauer G, Flandrin P (2011) A complete ensemble empirical mode decomposition with adaptive noise. Proceeding of the 36th International Conference on Acoustics, Speech and Signal Processing ICASSP 2011 (May 22-27, Prague, Czech Republic)

23. Colominas MA, Schlotthauer G, Torres ME (2014) Improved complete ensemble EMD: a suitable tool for biomedical signal processing. J Biomed Signal Process Control 14:19–29

24. Lei Y, Liu Z, Ouazri J, Lin J (2015) A fault diagnosis method of rolling element bearings based on CEEMDAN. Proc IMEchE C Mech Eng Sci 231(10):1804–1815

25. Bouhalais M, Djebala A, Ouelaa N, Babouri MK (2018) CEEMDAN and OWMRA as a hybrid method for rolling bearing fault diagnosis under variable speed. Int J Adv Manuf Technol 94(5–8):2475–2489

26. Ding F, Li X, Qu J (2017) Fault diagnosis of rolling bearing based on improved CEEMDAN and distance evaluation technique. J Vibroeng 19(1):1392–8716

27. Jing X, Jianmin M, Zhiqiang Z, Chun C (2019) Bearing fault diagnosis based on CEEMDAN and Teager energy operator. J Phys Conf Ser 1345:032044

28. An D, Xu B, Shao M, Li HD, Wang LY (2019) CEEMDAN-MFE method for fault extraction of rolling bearing. J Phys Conf Ser 1213:052092

29. Capdessus C, Sekko E, and Antoni J (2014) Speed transform, a new time-varying frequency analysis technique. Advances in condition monitoring of machinery in non-stationary operations. Springer Berlin, Heidelberg 23–35

30. Ait Sghir KA, Bolaers F, Cousinard O, Dron JP (2013) Vibratory monitoring of a spalling bearing defect in variable speed regime. Mech Industry 14(2):129–136

31. Wu TY, Lai CH, Liu DC (2016) Defect diagnostics of roller bearing using instantaneous frequency normalization under fluctuant rotating speed. J Mech Sci Technol 30(3):1037–1048

32. Pachaud C, Salvetat R, Fray C (1997) Crest factor and kurtosis contributions to identify defects inducing periodical impulsive forces. Mech Syst Signal Process 11(6):903–916

33. Dron JP, Bolaers F, Rasolofondraibe L (2004) Improvement of the sensitivity of the scalar indicators (crest factor and kurtosis) using a de-noising method by spectral subtraction: application to the detection of defects in ball bearings. J Sound Vib 270:61–73

34. Antoni J (2006) The spectral kurtosis: a useful tool for characterizing non-stationary signals. Mech Syst Signal Process 20(2):282–307